COMPARATIVE STUDY OF COHERENT VORTEX STRUCTURES IN A BOUNDARY LAYER WITH ADVERSE PRESSURE GRADIENT BY MEANS OF A NEW EXPERIMENTAL METHOD

V.I. Borodulin, Y.S. Kachanov, and A.P. Roschektayev

Institute of Theoretical and Applied Mechanics SB RAS,
630090 Novosibirsk, Russia

1. Introduction

A new method of experimental study of late nonlinear stages of laminar-turbulent transition is developed and applied for the case of a self-similar boundary layer with an adverse pressure gradient (APG). The paper concentrates on mechanisms of formation and development of coherent vortical structures and on comparison of their properties with those found earlier in the non-gradient (Blasius) boundary layer. Previous detailed experimental studies of nonlinear stages of transition in the APG case are restricted either by weakly-nonlinear stages [1-3] or by investigation of properties of turbulent spots excited "directly" by a strong pulse-like injections of air [4]. The present experiments were performed under controlled disturbance conditions. The formation of vortical structures is examined in the transition process initiated by a harmonic primary TS-wave, which initially is close to two-dimensional with a 3D admixture. In the case of the Blasius flow, these initial conditions correspond to the well-known K-regime of transition. The TS-wave was excited by a universal disturbance source developed in previous studies [5] and applied, for the first time, to investigation of late stages of the APG boundary-layer transition.

There are several kinds of coherent structures found in previous investigations in a transitional Blasius boundary layer (see [6] for review). Spikes, Λ-vortices, 3D high-shear layers, and ring-like vortices are among them. These structures were observed in experimental and numerical (DNS) investigations. Very similar flow patterns were also found in other transitional near-wall shear flows, such as the plane channel flow and the pipe flow, and also in the developed wall turbulence. Based on these observations, it was suggested in [6] that these structures are very *universal* and represent an inherent feature of the process of turbulence production in all near-wall flows in both transitional and turbulent regimes. Moreover, the mechanism of formation and interaction of these structures can be regarded as a *universal* mechanism of turbulence production. The main goal of the present study is to check this idea for the case of the APG boundary-layer transition, whose late stages have never been studied *experimentally* despite the great practical importance of this case. The only currently available study was performed *numerically* in [7] for a rather large APG (which is difficult to examine in the wind tunnel).

2. Basic Flow and Experimental Procedure

The experiment was conducted in the low-turbulence subsonic wind tunnel T-324 of the ITAM at the free-stream velocity $U_e \approx 9.0$ m/s. The wind tunnel has a 4 m long test section with a 1 m × 1 m cross-section. The free-stream turbulence level was below 0.02% in the frequency range above 1 Hz. The experimental setup (Fig. 1) was very similar to that used in [2, 3]. The boundary layer under investigation developed on a flat plate, which had a chord length of 1.49 m, a span of 0.99 m. The APG was induced over the plate by an adaptive wall-bump mounted on the test-section ceiling. The bump and the flap were adjusted in a way to have over the plate a streamwise APG, which would correspond to a fixed Hartree parameter $\beta_H = -0.115$. As shown in [8, 9], the basic flow structure both outside and inside the boundary layer is in a very good agreement with the theoretical one calculated by B.V. Smorodsky for this value of β_H. This fact is illustrated by the streamwise mean-velocity distribution measured outside the boundary layer at a distance $y = 10$ mm from the wall shown in Fig. 2. It is seen that the distribution agrees very well with that measured in [6] and calculated for $\beta_H = -0.115$.

Report Documentation Page

Report Date	Report Type	Dates Covered (from... to)
23 Aug 2002	N/A	-

Title and Subtitle Comparative Study of Coherent Vortex Structures in A Boundary Layer with Adverse Pressure Gradient by Means of A New Experimental Method	**Contract Number**
	Grant Number
	Program Element Number
Author(s)	**Project Number**
	Task Number
	Work Unit Number
Performing Organization Name(s) and Address(es) Institute of Theoretical and Applied Mechanics Institutskaya 4/1 Novosibirsk 530090 Russia	**Performing Organization Report Number**
Sponsoring/Monitoring Agency Name(s) and Address(es) EOARD PSC 802 Box 14 FPO 09499-0014	**Sponsor/Monitor's Acronym(s)**
	Sponsor/Monitor's Report Number(s)

Distribution/Availability Statement
Approved for public release, distribution unlimited

Supplementary Notes
See also ADM001433, Conference held International Conference on Methods of Aerophysical Research (11th) Held in Novosibirsk, Russia on 1-7 Jul 2002

Abstract

Subject Terms

Report Classification unclassified	**Classification of this page** unclassified
Classification of Abstract unclassified	**Limitation of Abstract** UU

Number of Pages
6

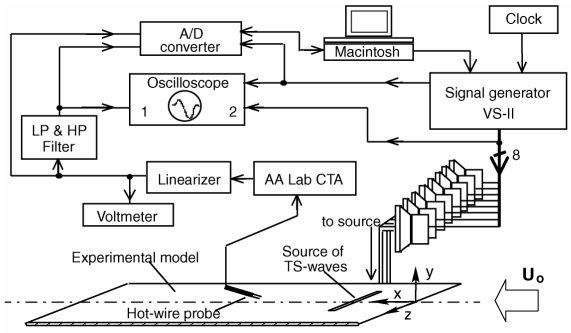

Fig. 1. Sketch of experimental setup.

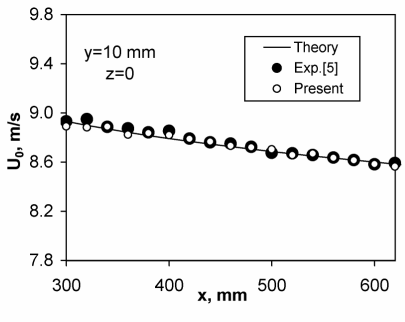

Fig. 2. Streamwise distributions of potential flow velocity.

The experiments were conducted at controlled disturbance conditions. The laminar-turbulent transition process was initiated by a harmonic (in time) primary TS-wave. The wave was excited by a universal disturbance source (see [5]) by means of weak blowing/suction air fluctuations through a plate-surface slit, which was perpendicular to the flow direction. The slit had a width of 0.8 mm and length of 164 mm. A block of 82 copper tubes (of 2 mm in diameter) was located on the bottom of the slit. The source was able to excite both 2D and 3D TS-waves with almost any desirable spanwise-wavenumber spectrum. Each tube was connected with a flexible plastic pipe to one of eight loudspeakers. The source was mounted at a distance x = 300 mm. The loudspeakers' input electric signals were generated by an electronic unit VS-II, which had eight channels and was controlled by a computer. The signals were formed by a computer program, downloaded into RAM of unit VS-II, and played back at rate controlled by an external clock. A reference signal had a frequency of repetition of the recorded realization and was used for the data acquisition system, in particular for the ensemble averaging of the hot-wire signals, which were linearized and introduced into an Apple computer via an A/D converter.

The main measurements were started at the 'initial' position $x = x_1 = 350$ mm where U_e = 8.8 m/s, the local Reynolds number $\mathrm{Re} = U_e\delta_1/\nu = 813$, the boundary layer displacement thickness $\delta_1(x_1) = 1.412$ mm, and the air kinematic viscosity $\nu = 1.528\cdot10^{-5}$ m^2/s. The excited primary (fundamental) TS-wave had frequency f_1 = 109.1 Hz. At the initial position this frequency corresponds to the frequency parameter $F = 2\pi f\nu/U_e^2\cdot10^6 = 135.2$. The wave was initially close to two-dimensional with a controlled primary 3D distortion discussed below.

The main measurements were conducted in the streamwise coordinate range x = 350 to 470 mm. The most detailed observations were performed in (y,z)-planes at five streamwise locations: x = 350, 400, 440, 449, and 461 mm (with $U_e(x)$ = 8.87, 8.80, 8.75, 8.74, and 8.73 m/s respectively), where five sets of wall-normal profiles were measured with spanwise steps from 6 to 0.7 mm and wall-normal steps from 0.05 to 1 mm. In every spatial point four mean values related to the streamwise flow velocity were recorded: (*i*) the mean velocity, (*ii*) the rms amplitude of total velocity fluctuations, (*iii*) the amplitude, and (*iv*) phase of the fundamental wave. The latter two values were obtained by Fourier analysis of the hot-wire time-series performed after their ensemble averaging for 10 to 20 signal realizations. Each realization consisted of 5 fundamental periods. In addition, the ensemble-averaged time-traces were also

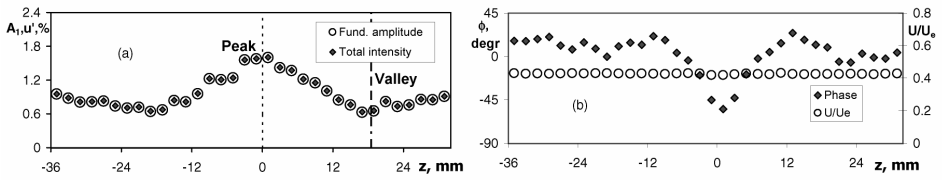

Fig. 3. Initial spanwise distributions of mean velocity and disturbance amplitudes and phases. x = 350 mm.

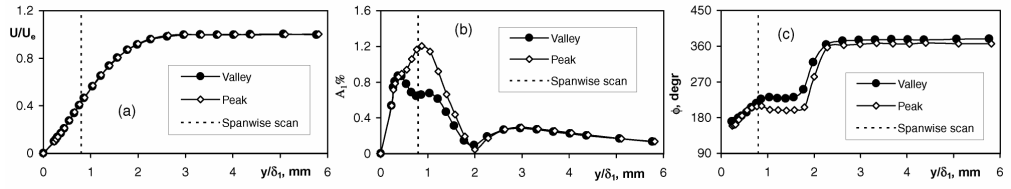

Fig. 4. y-profiles of mean velocity (*a*), disturbance amplitudes (*b*), and phases (*c*) at initial position. x = 350 mm.

recorded in every spatial point. These records were used for reconstruction of instantaneous velocity and vorticity fields and for subsequent 'visualization' of vortical flow structures, investigation of which represents the main goal of the present study.

3. Initial Perturbations

The initial disturbance conditions are illustrated in Figs. 3 and 4 for x =350 mm. The spanwise distributions of the fundamental-wave amplitude and phase shown in Fig. 3 were measured at a distance to the wall y = 1.14 mm (y/δ_1 = 0.792, U/U_e = 0.425) that was close to the TS-wave amplitude maximum in y-profiles (Fig. 4*b*). The spanwise modulation was arranged in a way to have somewhat higher amplitude and somewhat lower phase 'peak' position (z = 0) compared to those measured at the 'valley' position (z = 18.5 mm). This relatively weak modulation provoked further downstream formation of structures with their centers located in the peak position (see below).

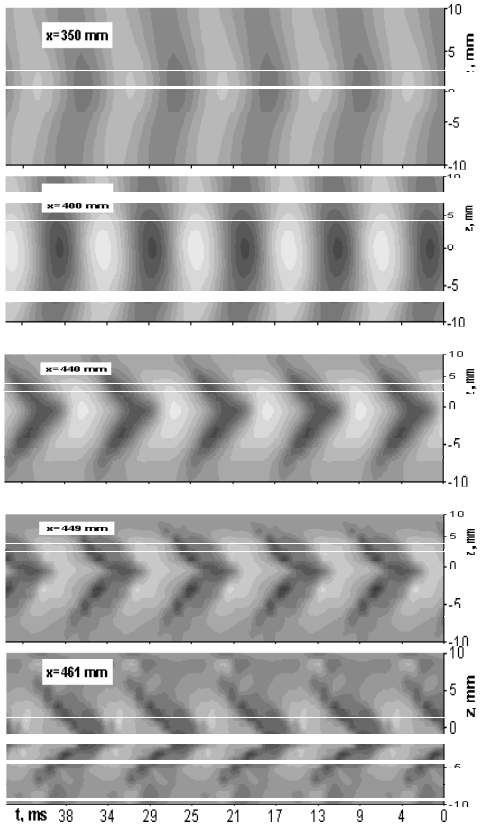

Fig. 5. Formation of structures in APG flow. Velocity disturbance. y = 1 mm.

At the initial streamwise position the shape of velocity time-traces is almost perfectly sinusoidal, therefore the fundamental-wave amplitude coincides completely with the total (in spectrum) disturbance intensity (Fig. 3*a*). The mean velocity distribution (Fig. 3*b*) does not display any significant basic flow distortion at this initial stage. The same thing is observed for other y-coordinates in two "initial" mean-velocity profiles measured at peak and valley positions (Fig. 4*a*). The fundamental-wave amplitude (Fig. 4*b*) and phase (Fig. 4*c*) profiles are qualitatively similar at these positions and have shapes quite typical for 2D TS-waves.

In case of Blasius boundary layer the initial disturbance conditions similar to those described above lead usually to the well-known K-regime of transition.

4. Formation of Λ-Structures

The process of formation of vortical structures is very well seen in Fig. 5, which shows contours of the instantaneous streamwise velocity disturbance u in ($-t$, z)-plane measured at five streamwise positions at a fixed distance from the wall y = 1.0 mm. Note, that the $-t$-axis can be regarded, in a certain sense, as the streamwise coordinate (under assumption that the structures are frozen within one fundamen-

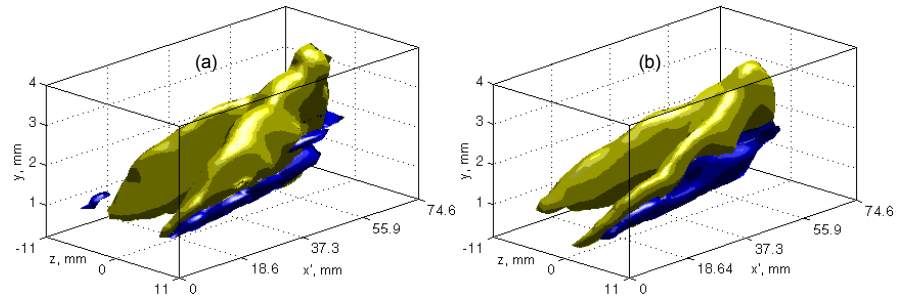

Fig. 6. Shapes of structures in APG (*a*) and Blasius (*b*) boundary layers. Contours of low value of total spanwise vorticity (black) and streamwise velocity disturbance (gray) in (*x′,y,z*)-space. x = 449 (*a*) and 450 (*b*) mm

tal period). The initially quasi-2D fronts of the TS-wave are distorted due to nonlinear interactions and form structures at x = 440 mm, which resemble very much famous Λ-structures previously observed in the Blasius flow. Further downstream their shape changes very little showing mainly stretching of the structures in the streamwise direction.

The real 3D shape of the structure observed at one-spike stage (x = 449 mm) is seen in Fig. 6*a* in (*x′,y,z*)-space, were $x' = -tU_e$. The replacement of time axis by coordinate x' is made in order to provide a comparability of the present data with those obtained in [10] for Blasius basic flow and to have the possibility to estimate some angular characteristics of the structures. There are two iso-surfaces shown in Fig. 6*a*: (*i*) the surface of constant (very small) instantaneous total spanwise vorticity $\overline{\Omega}_z = \Omega_z + \omega_z = \partial U/\partial y + \partial u/\partial y$ and (*ii*) the surface of constant (very low) instantaneous streamwise velocity disturbance u. As was found in previous experimental and numerical study [10] performed in the Blasius basic flow, the total spanwise vorticity has the lowest values (inside the boundary layer) in centers of the Λ-vortex 'legs'. Thus, low-level iso-surface of $\overline{\Omega}_z$ visualizes the Λ-vortex itself. Indeed, in the present APG boundary-layer case the shape of the corresponding iso-surface resemble Greek letter Λ very much The low-level iso-surface of u shows the region of the low-speed fluid, which has been displaced upward by an intensive rotation in the Λ-vortex 'legs'. This pattern also has the shape of Λ but it is positioned farther from the wall. The 3D high-shear layer is located even higher, on the top of this low-speed region (not shown in Fig. 6*a*). This layer separates the "original" high-speed fluid from the low-speed one "injected" upward by the Λ-vortex.

Very similar structures are observed in the Blasius flow transition. This fact is illustrated in Fig. 6*b* obtained by means of a post-processing of the experimental data [10] (for f_1 = 81.4 Hz and U_e = 9.18 m/s). Indeed, the shapes of both iso-surfaces are almost the same as in the APG case and, again, these are Λ-shapes. The relative positioning of the structures in space is also qualitatively similar and the angle of inclination of the APG Λ-vortex with respect to the wall is the same. However, the angle between two Λ-vortex 'legs' is larger by 8% compared to the Blasius case and the angle of inclination of the high-shear layer to the wall is greater by 15%. The former difference can be explained by a weaker stretching the Λ-vortex (due to lower mean-velocity gradient), the latter — by its more intensive rotation (due to stronger linear instability).

5. Spikes and Ring-Like Vortices

Different stages of development of the Λ-structures are clearly illustrated in Fig. 7, which presents contours of a kind of *projection* onto the wall of the low disturbance velocity. To make this projection, the *minimum* values of u have been chosen in every y-profile measured at every time moment and spanwise location. This kind of projection shows the shape of the structures in (*–t,z*)-plane; this is the Λ-shape. The structures in this presentation look, again, very similar to those detected in experiment and DNS [10] by means of the same projection (not shown). They become rather developed at x = 440 mm (Fig. 7) and then conserve

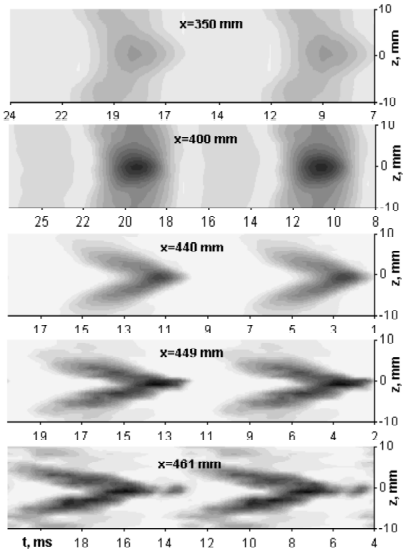

Fig. 7. Λ-structures in APG flow. Velocity disturbance minima in *y*-profiles.

approximately their shape displaying a stretching in the streamwise (–*t*) direction. At late stage (x = 461 mm) the formation of a localized region of low instantaneous velocity is observed ahead the Λ-structure tip in a qualitative agreement with the Blasius case studied in [10] (not shown). Figs. 8 and 9 show the shape of these late-stage structures in more detail.

A cross-section of the instantaneous streamwise velocity filed by a vertical plane (*–t,y*) in the peak position (z = 0) is presented in Fig. 8*a* for the APG case for x = 461 mm. The region of the low-speed fluid, located under the 3D high-shear layer, is seen very well. Ahead this region an isolated (rather small) low-speed spot is observed. Between these two regions a formation of the second small low-speed spot is also visible. This picture is again very similar to that obtained in the Blasius boundary-layer transition in [10] and presented in Fig. 8*b* (for a bit later stage of development). The x'-scale of the localized low-speed spots is practically the same in both cases.

The generation of spikes on time-traces is also observed in the APG boundary-layer transition in the vicinity of the peak position, similar to the Blasius case. Picture presented in Fig. 8*a* corresponds approximately to *two-spike stage*, while that shown in Fig. 8*b* — *three-spike stage.* The formation of spikes in the APG case is illustrated in Figs. 9 where the time-traces $u(t)$ are shown for five subsequent streamwise positions presented in Figs. 5 and 7. The sinusoidal, initially, shape transforms gradually into that with very sharp and intensive negative velocity fluctuations (the spikes), which number on every fundamental period increases downstream. At late stage (x = 461 mm) the spikes correspond to the localized regions of low instantaneous velocity displayed in Fig. 8*a*. In both cases (the APG and Blasius boundary layers) the amount of spikes observed at multi-spike stage depends, however, on distance from the wall. For example, in the case presented in Fig. 8*a*, there is only one spike at y = 4.0 mm, two spikes at y = 3.7 mm, and two and a half spikes at y = 3.4 mm (Fig. 9, x = 461 mm).

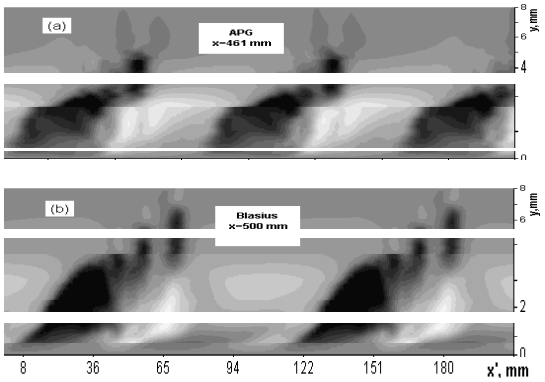

Fig. 8. Cuts of Λ-structures in APG flow at two-spike stage (*a*) and in Blasius flow (*b*) at three-spike stage. z = 0.

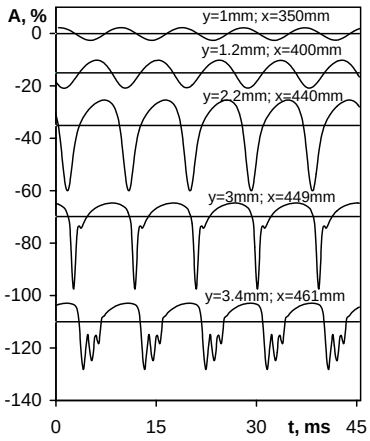

Fig. 9. Time-traces at peak position.

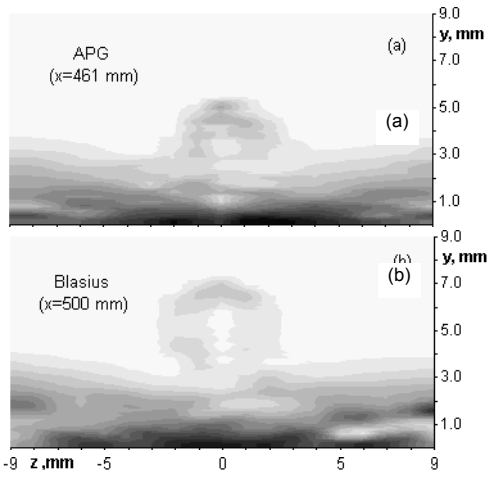

Fig. 10. Ring-like vortices at multi-spike stages.

As was clearly shown in [10] for the Blasius case, every spike (and low-speed spot) corresponds to a ring-like vortex detached from the Λ-vortex 'tip'. The ring-like vortex shape measured in [10] is presented in Fig. 10*b* in (*y*,*z*)-plane by means of iso-lines of gradient

$$\left|grad[u(y,z)]\right| = \sqrt{[\partial(U+u)/\partial y]^2 + [\partial(U+u)/\partial z]^2}$$

of the instantaneous total streamwise velocity in this plane. The picture corresponds to a time instant of the first spike. Very similar ring-like vortices turned out to exist in APG case (Fig. 10*a*). The spatial shape of the vortex is almost circular in both flows and the scale is almost the same. The vortex diameter is about 3 mm that is close to the boundary layer thickness.

6. Conclusions

A detailed experimental study of late nonlinear stages of transition, initiated in an APG boundary layer by a harmonic TS-wave, has been performed. Formation of Λ-vortices, Λ-shaped 3D high-shear layers, ring-like vortices, and spikes is found. All these structures are shown to be very similar to those found in previous experiments and DNS in the Blasius boundary layer. This result corroborates the idea discussed in [6] about existence of a universal mechanism of turbulence production in different wall bounded shear flows.

This work is supported by Russian Foundation for Basic Research (grant No. 00-01-00835).

REFERENCES

1. **Corke T., Gruber S.** Resonant growth of three-dimensional modes in Falkner-Skan boundary layers with adverse pressure gradients // J. Fluid Mech. 1996. Vol. 320. P. 211-233.
2. **Borodulin V.I., Kachanov Y.S., Koptsev D.B., Roschektayev A.P.** Resonant amplification of instability waves in quasi-subharmonic triplets with frequency and wavenumber detunings // Intern. Conf. on Methods of Aerophys. Research. Proc. Pt II. Novosibirsk,: 2002. P. 39-44ю
3. **Borodulin V.I., Kachanov Y.S., Koptsev D.B.** Experimental investigation of a resonant mechanism of amplification of continuous-spectrum disturbances in an APG boundary layer by means of a deterministic noise method // Intern. Conf. on Methods of Aerophys. Research. Proc. Pt I. Novosibirsk, 2002. P. 45-50.
4. **Seifert A., Wygnanski, I.J.** On turbulent spots in a laminar boundary layer subjected to a self-similar adverse pressure gradient // J. Fluid Mech. 1995 Vol. 296. P. 185-209.
5. **Borodulin V.I., Gaponenko V.R., Kachanov Y.S.** Method of introduction of normal instability modes into the 3D boundary layer // Intern. Conf. on Methods of Aerophy. Research. Proc. Pt 2. Novosibirsk, 1996. P. 39-45.
6. **Kachanov Y.S.** On a universal nonlinear mechanism of turbulence production in wall shear flows // Ibid., 2000, P. 84-91.
7. **Kloker M., Fasel H.** Numerical simulation of two- and three-dimensional instability waves in two-dimensional boundary layers with streamwise pressure gradient // Laminar-Turbulent Transition / Eds. D. Arnal, R. Michel. Berlin et al.: Springer-Verlag, 1990. P. 681.
8. **Kachanov Y.S. and Koptsev D.B.** Three-dimensional stability of self-similar boundary layer with a negative Hartree parameter. 1. Wave-trains // Thermophysics and Aeromechanics. 1999. Vol. 6, No. 4. P. 443-456.
9. **Kachanov Y.S. and Koptsev D.B., Smorodsky B.V.** Three-dimensional stability of self-similar boundary layer with a negative Hartree parameter. 2. Characteristics of stability // Ibid. 2000. Vol. 7, No. 3. P. 341-351.
10. **Borodulin V.I., Gaponenko V.R., Kachanov Y.S., Meyer D.G.W., Rist U., Lian Q.X., Lee C.B.** Late-stage transitional boundary-layer structures. Direct numerical simulation and experiment // Theoretical and Computational Fluid Dynamics. – 2002. Vol. 15. P. 317-337.